6-2016

Development and Validation of a Direct Tibial Loading Device for Mice

Sylvie Kalikoff
Union College - Schenectady, NY

Development and Validation of a Direct Tibial Loading Device for Mice

Sylvie Kalikoff

Introduction

Of the 6 million bones fractured each year in the United States, 5 to 10% do not heal properly [1]. Fractures range in severity and classification, and are therefore treated differently depending on the type of bone that was broken, the location of the break and the way in which the specific bone regrows. It is crucial that the appropriate treatment be carried out in order to properly heal the broken bone.

If a fracture does not heal correctly, it can result in a malunion, non-union, or delayed union. In the case of a malunion, the bony ends do not reconnect in an aligned, regular position [2]. This can result in a non-functional bone. In a non-union fracture, the bony ends do not meet and heal. Generally, nonunion fractures require surgery to fix. A delayed union is a fracture in which the bony ends do not reconnect in the amount of time it should take an average fracture to heal. This is dependent on the type and location of the break, but generally takes between 6 and 8 weeks [3].

The phases of fracture healing depend upon the stability of the bone during the healing process. A stable fracture results when the bony ends are held in place in order to decrease mobility and keep the bone aligned while it heals. This stability can come from external fixators, internal fixators, or a cast. Fixation uses pins and screws either inside or outside the body to hold the bony ends in place while the break heals (Figures 1 and 2).

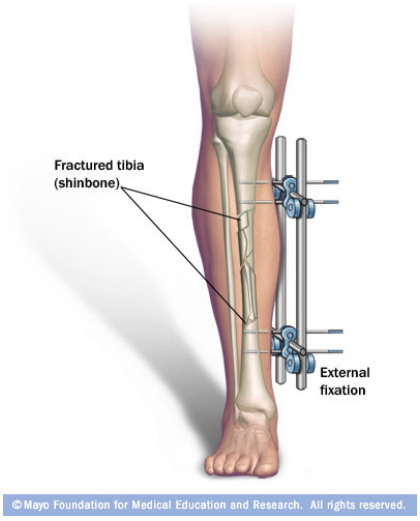

Figure 1: External fixation uses plates, pins, rods and screws to stabilize a broken bone from outside the body [4].

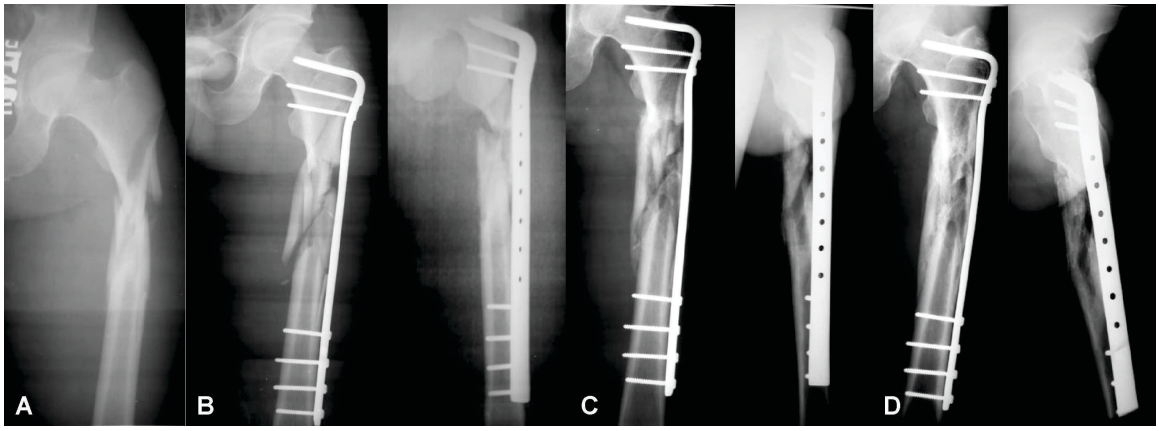

Figure 2: Internal fixation provides stability to a healing bone by surgically inserting plates, pins, rods and screws [5].

Intramembranous ossification occurs in stable fractures and begins when mesenchymal stem cells differentiate to form osteoblasts. Osteoblasts produce osteoid, which slowly gets mineralized between blood vessels to form trabeculae, which are small columns of bone. This is called woven bone, which gets further mineralized to form lamellar bone [6]. Lamellar bone is mature bone, and appears more organized than woven bone.

Unstable fractures heal through endochondral ossification. The first stage of endochondral ossification is inflammation, in which blood coagulates in a hematoma. Next, a soft callus forms, replacing the blood clot with granulation tissue and cartilage cells. This requires the differentiation of mesenchymal stem cells just as intramembranous ossification did, but into chondroblasts rather than osteoblasts. Chondroblasts form cartilage, which stabilizes the bony ends of the fracture, thereby allowing angiogenesis to occur. The cartilage of this soft callus gets calcified and woven bone forms, creating a hard callus. In a non-union fracture, the bone does not leave the soft callus phase. The last phase is called remodeling, which is an ongoing cycle of bone resorption and rebuilding by osteoclasts and osteoblasts respectively [7].

Previous studies have shown that the mechanical environment of a fracture plays a role in the healing process and rate. Smith Adaline et al. (2004) tested the effects of tensile and compressive forces on tissue formation in the fracture of a rat femoral model [8]. Fractures underwent mechanical stimulation three times per week for two weeks at a rate of 0.5 Hz for 17 minutes each session. Micro-CT showed an increase in bone formation in the areas of the fractures that experienced tension, and a lack of bone growth and cartilage formation in the areas that experienced compressive forces. This indicated that compression inhibits endochondral ossification, resulting in the lack of chondrogenesis and ultimately the inability of the fracture to heal. It is evident from this study that mechanical stimulation has varying effects on tissue development, which is helpful in

understanding what type of stimulation could be most beneficial for fracture healing.

Rontgen et al. (2010) also studied fracture healing in mice under various mechanical conditions. The effects of a flexible fixator that allowed for approximately 300 μm of motion and a rigid fixator that allowed for only about 14 μm of motion were compared. The ground reactive forces were measured pre and post-operatively with force plates on the bottom of the cages while the mice were able to roam freely. After 21 days it was determined using micro-CT and confirmed using histology that the fracture calluses in mice under flexible conditions were much larger than those under rigid conditions. A three-point bending test revealed lower bending stiffness in the flexible fixator group compared to the rigid fixator group. Woven bone, cartilage, and calluses were seen in mice under both conditions, although bony bridging was more complete in the fractures that experienced the rigid fixation. Since new bone and cartilage were present under flexible conditions even though the healing of the fracture was delayed, it is possible that adjustments to the flexible fixator to allow for slightly less motion could optimize the mechanical conditions for bone healing [9].

Claes et al. (2011) studied dynamization at various time points throughout the fracture healing process in a rat femoral model. One group of rats experienced rigid external fixation for three weeks and more flexible conditions for the last two weeks of the experiment through the removal of a locking bar. The second group of rats had the same rigid conditions for four weeks, and then experienced only one week under the more flexible conditions. These groups were compared to a control

group that experienced rigid conditions for the entire five weeks, and a control group that experienced flexible conditions for the entire five weeks. The experimental groups exhibited more advanced healing than either control group. A three-point bending test and micro-CT analysis showed that the group that experienced rigid conditions for four weeks had more elasticity and a smaller callus bone volume compared to the rigid fixation control group. This indicated that dynamization after bony bridging had begun may have increased the rate of healing, but when bony bridging had not yet begun, dynamization delayed new bone formation. Ultimately, the results of this study confirmed that late dynamization enhances fracture healing, but only once bony bridging has already begun [10].

Both Rontgen et al. and Claes et al. relied on weight bearing during ambulation as a means of stimulating the fracture. Although clinically translatable, it is difficult to study various loading protocols this way. Another technique to study the role of motion during fracture healing is through the direct loading of the bone. Our previous study hypothesized that the daily application of 150 μm of controlled, compressive motion to an external fixator on a 0.5mm tibial osteotomy would result in an increase in the rate of bone formation and a more mineralized fracture callus compared to a stable fracture [11]. The external fixator on the experimental group of mice was unlocked and attached to the linear actuator, which applied the 150 μm of compressive motion for 1 minute at a frequency of 1 Hz (Figure 3).

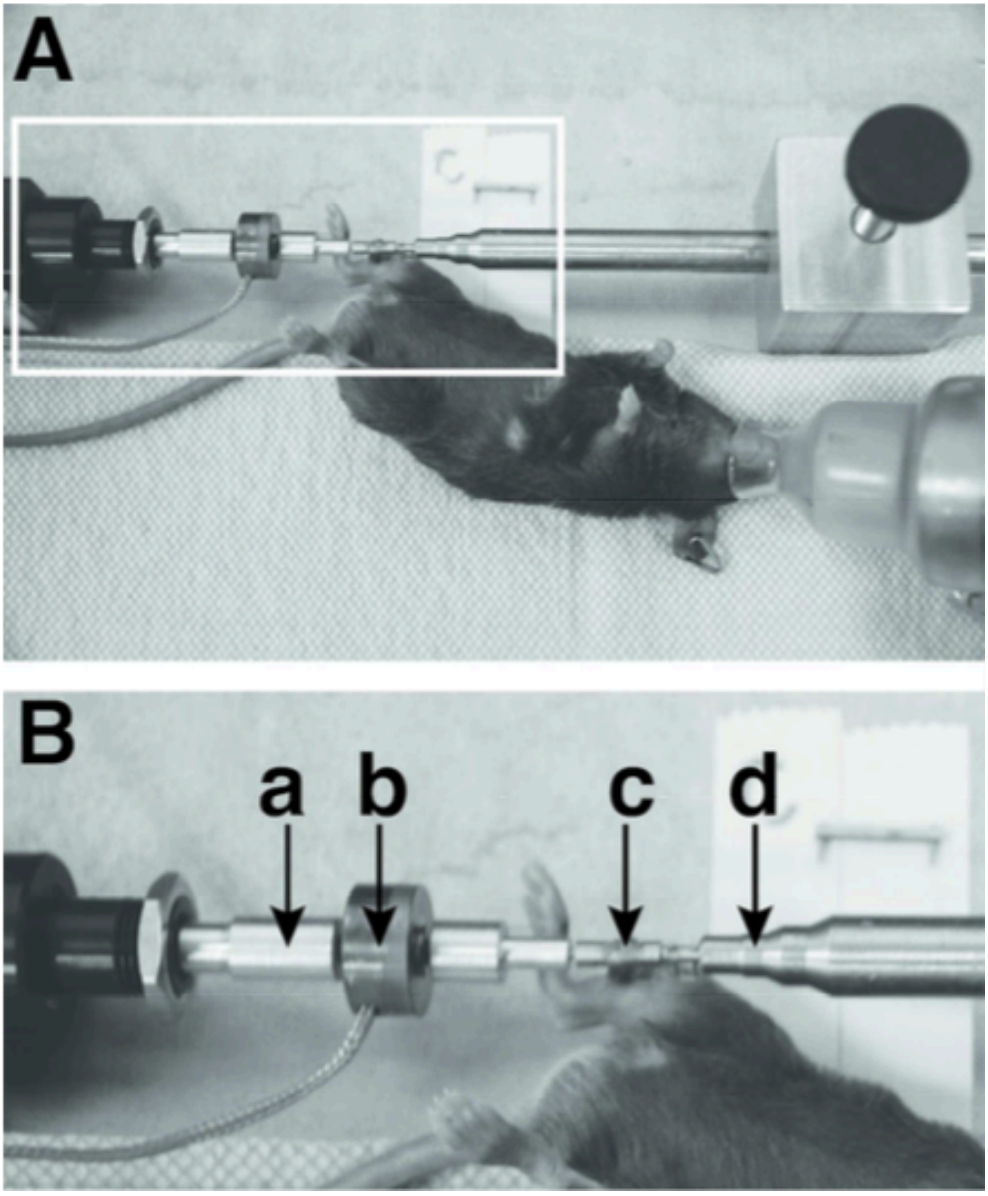

Figure 3: (A) Test set up with a mouse attached to the motion application system. (B) The system was comprised of a linear actuator (a) in series with a load cell (b) that displaced the distal component (c) of the fixator while the proximal component (d) was fixed.

The fixator remained locked in the control group to promote healing of a stable fracture. Control and experimental mice were euthanized 7, 12, 17, and 21 days post-operatively. Based on histology, micro-CT analysis, and statistical analysis, it was determined that there was not an increase in mineralized bone in

the fracture callus of mice that experienced controlled loading compared to control mice. Mineralized bone became apparent in both groups at the 21-day time point. Since both groups progressed to the hard callus stage of endochondral ossification, it was determined that the external fixator was of an appropriate rigidity to allow for weight bearing and to promote fracture healing. Although the optimal duration and magnitude of mechanical stimulation was not determined in this study, it was the first of its kind to implement mechanical stimulation to an external fixator of an open fracture in a mouse model.

Gardner et al. also directly loaded a mouse tibial model to study a different loading pattern. It was hypothesized that pause inserted loading "would lead to improvements in fracture healing compared with healing of nonloaded and repetitively loaded fractures, specifically in the early phases of healing" [12]. Pause inserted loading cycles have been shown to accelerate the rate of fracture healing. This is likely because there is a threshold at which increased load duration does not lead to increased bone mass. By inserting breaks into the loading, this threshold is never met, so bone mass can continue to increase. Mice underwent tibial osteotomies, which were stabilized with an intramedullary rod and nail. Loading was applied to an external device consisting of a cupped knee piece and a flat footplate (Figure 4).

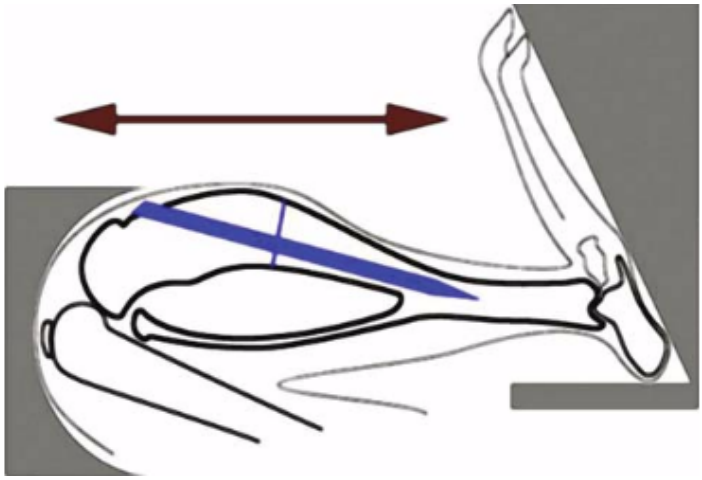

Figure 4: External loading device used to apply the load directly to the mouse rather than to a fixator.

One experimental group experienced loading without pause at a rate of 1 Hz for 100 cycles. The other experimental groups were time equivalent and cycle equivalent. The time equivalent group (100 seconds) experienced a 9 second pause, but only 10 cycles at a rate of 1 Hz. The cycle equivalent group experienced a 9 second pause and 100 cycles at a rate of 0.1 Hz. The control group did not experience loading. Advanced healing was seen earlier on in pause inserted groups and all three experimental groups had smaller callus volumes than the controls after 2 weeks of daily loading. This confirms that pause insertions were more effective in increasing bone mass in a healing fracture than steady loading without pause or no loading at all.

Physical activity is another method of directly loading the bone to study the affects of mechanical stimulation on fracture healing. Stadelmann et al. compared the experimental designs of physical activity and axial compression in mouse tibiae [13]. While exercise is clinically relevant, the strains involved are not as easily controlled as in axial compression. In designing a study using treadmill running, an

acclimation period in which the animal is given direction is necessary to familiarize the animal with the treadmill. Sometimes, electrical shocks are used to induce running. After a week of acclimation, running can begin. The factors that can be controlled on a treadmill are inclination, duration of physical activity, and speed, and they determine the changes in bone health due to activity level. In direct loading through axial compression, the loading waveform shape, frequency, number of cycles, number of pauses, and strain rate all have an affect on the remodeling that occurs during loading. There is not a general consensus on the loading waveform parameters that are best suited for bone growth, but it has been shown that higher strain rates result in increased bone formation. The force applied to the bone determines the strain rates. Although there are limitations associated with each method, both axial compression and exercise are effective ways of applying mechanical stimulation to a healing fracture or healthy bone.

Methods

Since the loading of a tibial osteotomy to an external fixator was not successful in increasing the rate of fracture healing, a motion application system was designed to apply direct loading to the mouse tibia. The system (Figure 5) consists of a linear actuator (T-NA micro linear actuator, Zaber Technologies, Inc., Vancouver, BC) connected in series with a load cell (Transducer Techniques, Telemecula, CA model MDB-2.5). The linear actuator applies the load to the ankle through a removable ankle platen, which is in line with a removable knee platen that connects to the load cell. The mouse tibia sits between the ankle and knee platens.

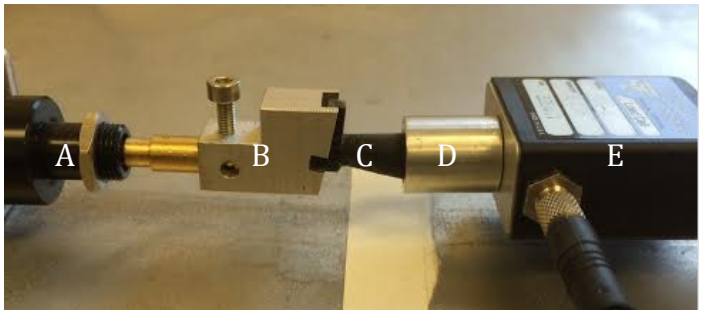

Figure 5: Motion application system with linear actuator (A), ankle platen (B), phantom leg (C) knee platen (D), and load cell (E).

Zaber Console was used to program the linear actuator to move forward and backward 75 µm at a rate of 1 Hz for 1 minute. The code records the displacement of the linear actuator approximately every 1/63 of a second throughout loading. The displacement data is automatically saved into a file that writes over itself after each run.

LabVIEW 2012 was used to collect data from the load cell and data acquisition system (NI 9237, National Instruments, Austin, TX). The DAQ Assistant was wired to a waveform function to collect the force data in Newtons from the load cell and data acquisition system (Figure 6).

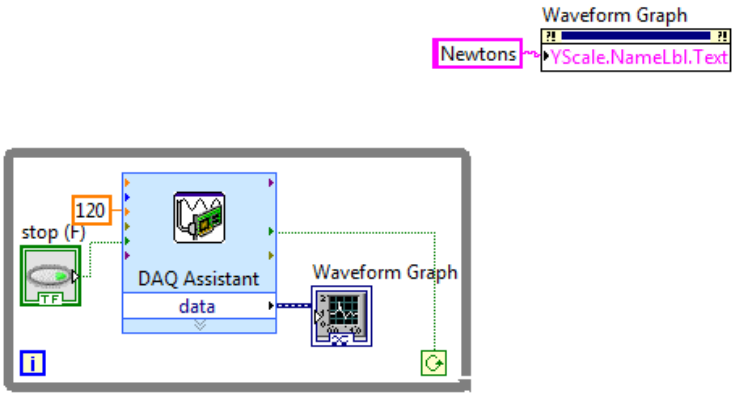

Figure 6: Block diagram of the LabVIEW program used to collect force data.

In order to validate the data acquisition and motion application systems, a model of a mouse leg below the knee was designed in Solidworks. Four phantom legs were 3D-printed on an Objet Connex 500 printer. Different combinations of TangoPlus FLX930 and VeroWhitePlus RGD835 were used to create four phantom legs, each of a different, known shore hardness (Figure 7) [14]. Leg 1 was FLX9885 with a shore hardness (A) of 80-85, making it the most stiff. Leg 2 was FLX9850 with a shore hardness (A) of 45-50. Leg 3 was FLX9860 with a shore hardness (A) of 57-63. Leg 4 was pure TangoPlus with a shore hardness (A) of 26-28, making it the least stiff and most flexible leg.

Figure 7: 3D-printed leg of Tango Plus FLX930 with a shore hardness of 27.

Shore hardness can be converted to Young's Modulus (Equation 1) [15].

Equation 1: $$E = e^{(((shore\ A\ durometer)*0.0235)-0.6403)}$$

where E is the Young's Modulus.

To confirm that the load cell and linear actuator both provide accurate data, a stress strain curve was created to determine the experimental Young's Modulus (Equation 2).

Equation 2: $$E = \frac{\sigma}{\varepsilon}$$

where E is Young's Modulus, σ is stress, and ε is strain.

The phantom leg was loaded and the displacement information from Zaber was used to determine the strain on the leg (Equation 3).

$$\textbf{Equation 3:} \quad \boldsymbol{\varepsilon} = \frac{\Delta \boldsymbol{L}}{\boldsymbol{L}}$$

where ε is strain, ΔL is the change in length of the leg, and L is the total length of the leg.

LabVIEW was used to gather the force data, and Microsoft Excel was used to calculate the stress on the ankle, mid-leg and upper leg (Equation 4).

$$\textbf{Equation 4:} \quad \sigma = \frac{F}{A}$$

where σ is stress, F is force, and A is cross sectional area.

Cross sectional areas were 17.35, 25.74, and 36.96 mm^2 respectively. A calibration curve was created with weights of known values to determine any inconsistencies between LabVIEW data and the actual values.

Results and Discussion

The calibration curve determined a consistent offset of about 2.27 Newtons on LabVIEW. Also, each value was off by 10%. The force data was collected into a waveform graph of force (Newtons) vs. time (seconds) (Figure 8).

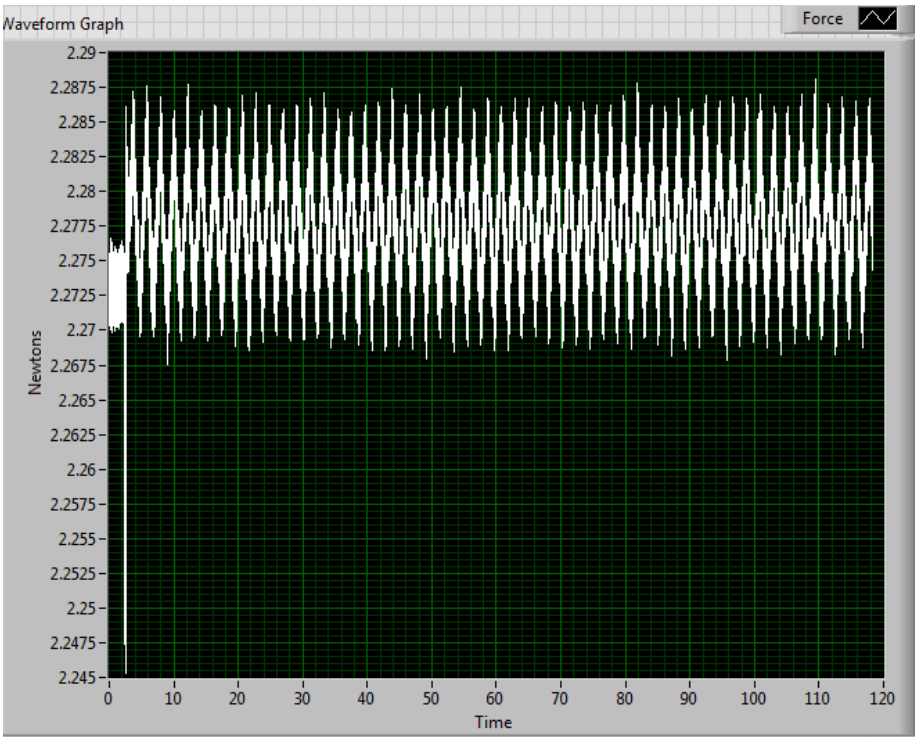

Figure 8: Force vs. Time waveform graph on Labview based on 300um of displacement of the linear actuator on Zaber on Leg 4.

The offset of 2.27 was subtracted from the force data, which was then multiplied by 10 to make up for the 10% error. Stress and strain curves were created for 75 um, 150 um and 300 um of displacement. At 75um the data was not consistent or logical, likely because the low levels of motion were not in the scope of the load cell. At 150 um, the experimental Young's Moduli of Leg 4 ranged from 6 MPa to 9 MPa, with an average of 8.33 MPa and an n of 6. At 300 um, the experimental Young's Moduli ranged from 3 MPa to 7 MPa, with an average of 4.5 MPa. The known Young's Modulus of Leg 4 is approximately 1MPa. As the cross sectional area of the phantom leg increased, the experimental Young's Modulus decreased and was more accurate.

This high error can be attributed to a variety of sources. Firstly, the load cell is most accurate when it works in its mid range. It is evident that the data is more

accurate when there is greater motion. With a displacement of 75 um, the load cell was picking up less than 1 lb of force, which is at the very low end of the 5-lb range of the load cell. When there is increased motion and increased force, the load cell is gets more accurate results. It is also possible that since the leg is an irregular shape, the loading is not exactly linear, leading to some error.

Future Work

The motion application system can be used to apply controlled, axial *in vivo* loading to a mouse tibia in an effort to understand the effects of mechanical loading on bone health. The frequency and duration of loading as well as the pattern of the loading waveform are still being studied and have yet to be determined. After validation, the system can be used to further explore the affects of direct loading of the tibia.

The system is mounted on a stage that can be modified for other mechanical tests such as bending tests. The stage can be rotated 90° vertically so that the linear actuator provides vertical movement rather than horizontal movement. The ankle and knee platens can be removed from the linear actuator and load cell respectively. They can be replaced with prongs for three- and four-point bending tests. Since the linear actuator would be applying the forces from above, two replaceable parts would be created to fit the actuator tip. One part would have just one prong for three-point bending (Figure 9). The other part would have two prongs for four-point bending (Figure 10).

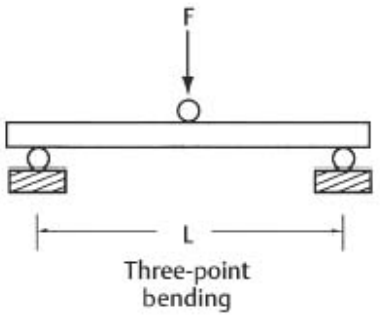

Figure 9: Mechanical setup for three-point bending tests [16].

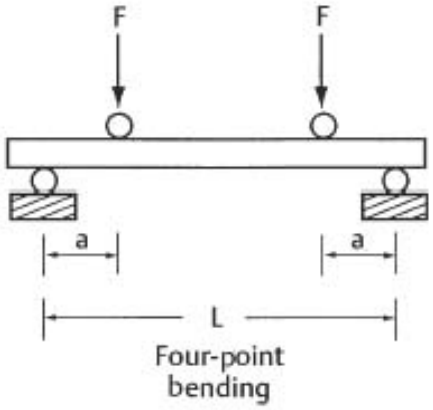

Figure 10: Mechanical setup for four-point bending tests [16].

The support span, L, between bottom prongs would remain constant in both three- and four- point bending tests. Previous studies have used a variety of values for the support span. Shriefer et al. (2005) use a span of 11.2mm for three-point bending of the tibia [17]. Bhatia & Troy (2012) use a span of 7mm in a similarly designed tensile stage for mechanical testing, however they performed bending tests in multiple locations along the tibia [18]. These variations may be due to the inconsistent curve of the tibia. When an appropriate span has been determined, bending tests allow the strength of bone to be analyzed. With physical activity as

another form of mechanically stimulating bone, the ability to perform bending tests could lead to future experiments on the affects of exercise on bone strength.

References

[1]Physical Fields. (2002, October). Retrieved June 02, 2016, from http://orthoinfo.aaos.org/topic.cfm?topic=A00279

[2] Pugh, K. J., & Rozbruch, S. R. (n.d.). Malunions and Nonunions. *American Academy of Orthopaedic Surgeons: Orthopaedic Knowledge Update, Trauma 3*, 115-130.

[3] Nunamaker, D. M., Rhinelander, F. W., & Heppenstall, R. B. (n.d.). Delayed Union, Nonunion, and Malunion. Retrieved June 02, 2016, from http://cal.vet.upenn.edu/projects/saortho/chapter_38/38mast.htm

[4] External Fixation. (n.d.). Retrieved June 02, 2016, from http://www.mayoclinic.org/diseases-conditions/broken-leg/multimedia/external-fixation/img-20005996

[5] Minimally Invasive Plate Osteosynthesis (MIPO) in Long Bone Fractures – Biomechanics – Design – Clinical Results. (2011). Retrieved June 02, 2016, from http://www.intechopen.com/books/biomechanics-in-applications/minimally-invasive-plate-osteosynthesis-mipo-in-long-bone-fractures-biomechanics-design-clinical-res

[6] Cumming, B. (2006). Stages of Intramembranous Ossification. Retrieved from http://www.kean.edu/~jfasick/docs/Fall Semester Lectures Chapt. 1-15 '07/Chapter 6B.pdf

[7] Ross, M. H., & Pawlina, W. (2006). *Histology: A Text and Atlas* (5th ed.). Baltimore, MD: Lippincott Williams & Wilkins.

[8] Smith-Adaline, E. A., Volkman, S. K., Ignelzi, M. A., Slade, J., Platte, S., & Goldstein, S. A. (2004). Mechanical environment alters tissue formation patterns during fracture repair. *Journal of Orthopaedic Research J. Orthop. Res., 22*(5), 1079-1085. doi:10.1016/j.orthres.2004.02.007

[9] Röntgen, V., Blakytny, R., Matthys, R., Landauer, M., Wehner, T., Göckelmann, M., . . . Ignatius, A. (2010). Fracture healing in mice under controlled rigid and flexible conditions using an adjustable external fixator. *Journal of Orthopaedic Research J. Orthop. Res., 28*(11), 1456-1462. doi:10.1002/jor.21148

[10] Claes, L., Blakytny, R., Besse, J., Bausewein, C., Ignatius, A., & Willie, B. (2011). Late Dynamization by Reduced Fixation Stiffness Enhances Fracture Healing in a Rat Femoral Osteotomy Model. *Journal of Orthopaedic Trauma, 25*(3), 169-174. doi:10.1097/bot.0b013e3181e3d994

[11] Currey, J. A., Mancuso, M., Kalikoff, S., Miller, E., & Day, S. (2015). Controlled Cyclic Compression of an Open Tibial Fracture Using an External Fixator Affects Fracture Healing in Mice. *Journal of Biomechanical Engineering J Biomech Eng, 137*(5), 051011. doi:10.1115/1.4029983

[12] Gardner, M. J., Ricciardi, B. F., Wright, T. M., Bostrom, M. P., & Marjolein C. H. Van Der Meulen. (2008). Pause Insertions During Cyclic In Vivo Loading Affect Bone Healing. *Clinical Orthopaedics and Related Research Clin Orthop Relat Res, 466*(5), 1232-1238. doi:10.1007/s11999-008-0155-1

[13] Stadelmann, V. A., Brun, J., & Bonnet, N. (2015). Preclinical mouse models for assessing axial compression of long bones during exercise. *BoneKEy Rep BoneKEy Reports, 4*, 768. doi:10.1038/bonekey.2015.138

[14] Digital Materials Data Sheet. (n.d.). Retrieved from http://usglobalimages.stratasys.com/Main/Files/Material_Spec_Sheets/MSS_PJ_DigitalMaterials_Datasheet.pdf?v=635832868828035876

[15] Convert Durometer to Young's Modulus. (n.d.). Retrieved June 10, 2016, from https://www.3dvision.com/blog/entry/2011/07/14/convert-durometer-to-youngs-modulus.html

[16] Brantley, W. A., Eliades, T., & Litsky, A. S. (n.d.). 2 Mechanics and Mechanical Testing of Orthodontic Materials. Retrieved June 10, 2016, from http://pocketdentistry.com/2-mechanics-and-mechanical-testing-of-orthodontic-materials/

[17] Schriefer, J. L., Robling, A. G., Warden, S. J., Fournier, A. J., Mason, J. J., & Turner, C. H. (2005). A comparison of mechanical properties derived from multiple skeletal sites in mice. *Journal of Biomechanics, 38*(3), 467-475. doi:10.1016/j.jbiomech.2004.04.020

[18] Bhatia, V., & Troy, K. (2012). A Portable Small-Scale Mechanical Loading and Testing Device: Validation and Application to a Mouse Tibia Loading Model. *Experimental Techniques Exp Techniques, 39*(4), 3-8. doi:10.1111/j.1747-1567.2012.00843.x